HHS Public Access

Author manuscript

Nat Cell Biol. Author manuscript; available in PMC 2014 May 01.

Published in final edited form as:

Nat Cell Biol. 2013 November ; 15(11): 1362–1369. doi:10.1038/ncb2862.

Heart field origin of great vessel precursors relies on *nkx2.5*-mediated vasculogenesis

Noëlle Paffett-Lugassy[1,2,3], **Reena Singh**[4], **Kathleen R. Nevis**[1,2], **Burcu Guner-Ataman**[1,2], **Evan O'Loughlin**[1,2], **Leila Jahangiri**[1,2], **Richard P. Harvey**[4], **C. Geoffrey Burns**[1,2,3,*], and **Caroline E. Burns**[1,2,3,*]

[1]Cardiovascular Research Center, Massachusetts General Hospital, Charlestown, MA 02129

[2]Harvard Medical School, Boston, MA 02115

[3]Harvard Stem Cell Institute, Cambridge, MA 02138

[4]Victor Chang Research Institute, Darlinghurst, New South Wales, 2010, Australia

Abstract

The pharyngeal arch arteries (PAAs) are transient embryonic blood vessels that make indispensable contributions to the carotid arteries and great vessels of the heart, including the aorta and pulmonary artery[1, 2]. During embryogenesis, the PAAs appear in a craniocaudal sequence to connect pre-existing segments of the primitive circulation after *de novo* vasculogenic assembly from angioblast precursors[3, 4]. Despite the unique spatiotemporal characteristics of PAA development, the embryonic origins of PAA angioblasts and the genetic factors regulating their emergence remain unknown. Here, we identify the embryonic source of PAA endothelium as *nkx2.5*$^{+}$ progenitors in lateral plate mesoderm long considered to adopt cell fates within the heart exclusively[5, 6]. Further, we report that PAA endothelial differentiation relies on Nkx2.5, a canonical cardiac transcription factor not previously implicated in blood vessel formation. Together, these studies reveal the heart field origin of PAA endothelium and attribute a novel vasculogenic function to the cardiac transcription factor *nkx2.5* during great vessel precursor development.

During the course of analyzing zebrafish embryos expressing a yellow fluorescent protein from *nkx2.5 cis*-regulatory sequences [*Tg(nkx2.5:ZsYellow)*][7], we observed fluorescence in known *nkx2.5*$^{+}$ organs including the heart and liver (Fig. 1a and Supplementary Fig. 2a). Unexpectedly, we also observed ZsYellow fluorescence in pharyngeal structures revealed

*Corresponding authors: CGB (gburns@cvrc.mgh.harvard.edu) and CEB (cburns6@partners.org).

Supplementary Information is linked to the online version of the paper at www.nature.com/ncb.

Author Contributions N.P.L. designed and performed the zebrafish experiments, analyzed data, and co-wrote the paper; R.S. designed, performed, and analyzed the mouse experiments, and co-wrote the paper; C.G.B. and B.G.A. created the *Tg(nkx2.5:CreER*^{T2}*)* and *Tg(nkx2.5:nZsYellow)* lines; K.R.N., E.O., and L.J. performed and analyzed zebrafish experiments; R.P.H. analyzed data, designed experiments, and co-wrote the paper; C.G.B. and C.E.B. initiated and directed the study, analyzed data, and co-wrote the paper with input from all authors.

Author Information The authors declare no competing financial interests.

through co-localization studies to be endothelial cells comprising PAAs 3-6 and the adjoining ventral aorta (VA; Fig. 1a-d). Among the embryonic vasculature, only the PAAs and VA expressed ZsYellow consistent with their unique developmental origin[3, 4]. To pursue this observation further, we followed the dynamics of ZsYellow fluorescence during developmental stages leading up to PAA establishment. During mid-somitogenesis, we observed ZsYellow in bilateral populations of anterior lateral plate mesoderm (ALPM) previously identified as ventricular myocardial precursors in the zebrafish heart forming region[6, 8] (Fig. 1e; Supplementary Fig. 2b, c; Supplementary Fig. 2g-j). As expected, ventricular precursors migrated medially and contributed to the heart. Interestingly, fractions of the ZsYellow$^+$ field remained lateral and condensed by 28 hours post-fertilization (hpf) into pharyngeal clusters (Fig. 1f, g) that we verified were non-endodermal (Fig. 1h; Supplementary Fig. 2d-f).

To rule out a position effect of the transgene, we confirmed that *nkx2.5* transcripts also localized to pharyngeal clusters at 28 hpf (Fig. 1i; SupplementaryFig. 2k, l). Over the next 20 hours, however, *nkx2.5* transcipts progressively disappeared in a craniocaudal sequence until expression was undetectable specifically in the pharynx at 48 hpf (Fig. 1j-l; Supplementary Fig. 2m, o). By contrast, ZsYellow transcripts persisted longer in *Tg(nkx2.5:ZsYellow)* embryos, thereby providing an explanation for the robust ZsYellow fluorescence observed in PAAs 3-6 (Supplementary Fig. 2n-p). Intriguingly, a previous report[3] described the cranial to caudal appearance of four *tie1*$^+$ PAA angioblast clusters in pharyngeal mesoderm during a developmental window overlapping with the cranial to caudal disappearance of *nkx2.5*$^+$ clusters that we observed (Fig. 1j-l). Using double *in situ* hybridization, we revealed a reciprocal relationship between *nkx2.5* and *tie1* transcripts in each pharyngeal cluster (Fig. 1m-p). Specifically, *nkx2.5* expression precedes that of *tie1* (Fig. 1m), yet after a transient period of overlap, *nkx2.5* transcripts decline while *tie1* expression is maintained throughout PAA morphogenesis[3] (Fig. 1n-p). These data suggest that *tie1*$^+$ PAA angioblasts derive from undifferentiated *nkx2.5*$^+$ clusters in the pharynx.

To begin testing this hypothesis, we tracked the derivatives of *nkx2.5*$^+$ clusters expressing the photoconvertible Kaede protein, which instantly switches from green to red fluorescence following ultraviolet (UV) light exposure[9]. Pan Kaede photoconversion at 30 hpf resulted in robust red fluorescence in PAAs 3 and 4 with regions of red and green fluorescence or green-only fluorescence in PAAs 5 and 6 (Fig. 2a-d). Based on the red and green fluorescent signal distributions, we conclude that PAAs 3 and 4 derive exclusively from progenitor cells that express *nkx2.5* prior to photoconversion at 30 hpf. By contrast, only a small fraction of PAAs 5 and 6 derive from cells expressing *nkx2.5* prior to photoconversion with the majority of progenitors initiating *nkx2.5* expression thereafter.

To test if each *nkx2.5*$^+$ cluster gives rise to a single PAA, we individually traced their cell fates using focused Kaede photoconversion. At 30 hpf, three bilateral pairs of *nkx2.5*$^+$ clusters were visualized in pharyngeal mesoderm (Fig. 2e). The second cluster gives rise exclusively to PAA3 (Fig. 2e, f). The third cluster, and scattered cells located caudal to the third cluster, become PAA4 and part of PAA5 (Supplementary Fig. 3a-c). Between 30 and 44 hpf, we witnessed the caudal emergence of two new Kaede clusters that when photoconverted individually, resulted in PAAs 5 or 6 being labeled exclusively with red

fluorescence (Fig 2g, h). These findings support our hypothesis that individual *nkx2.5*$^{+}$ clusters give rise to single PAAs and that the majority of progenitors for the caudal-most PAAs are specified after 30 hpf.

Based on the apparent segregation of ZsYellow^{+} pharyngeal clusters from myocardial precursors in the ALPM of *Tg(nkx2.5:ZsYellow)* embryos (Fig. 1e-g), we hypothesized that PAA endothelium derives from *nkx2.5*$^{+}$ progenitors located in the classically defined heart forming region, a population long considered to adopt cell fates within the heart exclusively[5, 6, 10]. We tested this hypothesis by employing two complementary lineage tracing strategies. First, using tamoxifen-inducible Cre/loxP lineage tracing, we transiently induced Cre activity in *nkx2.5*$^{+}$ cells for two hours during heart field stages (Supplementary Fig. 3j) and identified their derivatives using endothelial restricted [*Tg(kdrl:CSY)*][7] or ubiquitous [*Tg(ubi:Switch)*][11] Cre-responsive "color switching" reporters. Remarkably, we observed scattered reporter labeling of endothelial cells within PAAs 3-6 and the VA (Fig. 2i,j; Supplementary Fig. 3k-n). The majority of animals exhibited reporter fluorescence in PAAs 3 and 4 with lower percentages reporting fluorescence in PAAs 5 and 6 (Fig. 2j; Supplementary Fig. 3o).

In a complementary approach, we photoconverted Kaede protein unilaterally in left-side *nkx2.5*$^{+}$ heart field progenitors and observed red fluorescence throughout left-side PAAs 3 and 4 with markedly weaker signal in caudal PAAs 5 and 6 (Fig. 2k,l). As an internal control, PAAs residing contralaterally failed to express red fluorescence (Supplementary Fig. 3d-f). Furthermore, pan-photoconversion of *nkx2.5*$^{+}$ heart field cells labelled not only the heart tube, but the three pharyngeal clusters and scattered posterior cells present at 30 hpf (Supplementary Fig. 3g-i). Taken together, these data from Kaede photoconversion and Cre/loxP lineage tracing demonstrate that *nkx2.5*$^{+}$ progenitors residing in the zebrafish heart field give rise to PAA endothelium. Further, the decline in labeling efficiency observed in PAAs 5 and 6 supports our previous observation that these caudal vessels derive from progenitor cells that initiate *nkx2.5* expression in the ALPM and those that are specified subsequently in pharyngeal mesoderm (Fig. 2a-h).

PAA establishment appears qualitatively similar across vertebrate species as each PAA forms in a craniocaudal sequence[12, 13] through the assembly of nascent angioblasts into discrete vessels[3, 4]. Although the progenitor source of these angioblasts has not been defined, a previous Cre recombinase-based lineage tracing study noted descendants of *Nkx2-5*-expressing cells in endocardium as well as putative endothelial cells scattered throughout the first pharyngeal arch[14]. However, PAAs were not systematically examined, and in the absence of co-labeling studies and high resolution imaging, the molecular identity of the traced cells remains unclear. To conclusively determine if PAA endothelium in the mouse derives from *Nkx2-5*$^{+}$ progenitors, we performed Cre/loxP lineage tracing using the previously characterized *Nkx2-5*^{IRESCre} driver[14] with the *Z/EG*[15] or *ROSA*^{YFP}[16] reporters followed by immunostaining with the endothelial cell marker PECAM1. As anticipated, robust reporter expression was observed in the myocardium and endocardium of the heart (Supplementary Fig. 3p, q)[14]. Strikingly, reporter fluorescence at E9.5 and E10.5 co-localized with PECAM1 in PAAs 1 and 2, respectively (Fig. 2p; Supplementary Fig. 3r,s). At later stages, reporter fluorescence was also observed in PAAs 3, 4, and 6 (Fig. 2m-p;

Supplementary Fig. 3t), the embryonic vessels that generate critical segments of the postnatal carotid arteries, aorta, and pulmonary artery, respectively[12, 17]. Rare overlap was also observed in the dorsal aorta (DA) endothelium at the sites of PAA attachment (Fig. 2o ′). These findings highlight the evolutionary conservation of PAA endothelial cell derivation from an *Nkx2-5*$^{+}$ source in mammals.

To assess the requirement for *nkx2.5* during PAA establishment in zebrafish, we employed a previously validated anti-sense morpholino[18] to suppress Nkx2.5 function (Supplementary Fig. 4a,b). While control embryos exhibited strong blood flow through PAAs 3-6 (Fig. 3a), *nkx2.5* morphants displayed either a reduction in PAA number (class I; Fig. 3b) or absence of PAAs altogether (class II; Fig. 3c). Importantly, PAA1, which establishes the initial circulatory loop in zebrafish, develops much earlier in an *nkx2.5*-independent manner (Fig. 1p)[13, 19]. As such, both morphant classes maintained robust blood flow through the remaining vasculature reducing the likelihood that hemodynamic alterations caused the observed phenotype. Consistent with this idea, PAA vasculogenesis occurs normally in *silent heart* mutants that completely lack heart function and blood flow[20].

Compared to control mouse embryos that displayed well-formed PAAs 1-3 at E9.5 (Fig. 3d), *Nkx2-5*$^{lacZ/lacZ}$ null animals exhibited either disrupted PAAs with residual mis-patterned endothelial cells (Fig. 3e) or a complete absence of PAAs altogether (Fig. 3f; Supplementary Fig. 4g-i). While ink injections in wild-type embryos revealed patent cardiac outflow tracts (OFTs) with prominent forward flow into the paired PAA3 vessels (Fig. 3i), the OFTs in *Nkx2-5*$^{lacZ/lacZ}$ mutants ended in a blind sac (Fig. 3j). These data demonstrate a previously unappreciated requirement for Nkx2-5 in PAA establishment that is conserved from zebrafish to mammals.

To elucidate the cellular mechanism underlying the PAA defect in Nkx2.5-deficient zebrafish, we evaluated *nkx2.5* morphants for PAA progenitor cell specification and differentiation. Using a transgenic strain that highlights *nkx2.5*$^{+}$ nuclei, we documented equivalent numbers of *nkx2.5*$^{+}$ progenitors in control and morphant heart fields (Supplementary Fig. 4j-l), indicating proper specification. Examination of fluorescence in morpholino-injected *Tg(nkx2.5:Kaede)* embryos revealed that PAA progenitor cells also clustered properly by 30 hpf (Fig. 4a,d). Photoconversion of kaede expressed within morphant clusters revealed that they were maintained properly in the pharynx, but failed to form organized vessels, suggesting that Nkx2.5 is required specifically for PAA vasculogenesis (Fig. 4b,c,e,f). Next, we evaluated morphants for *nkx2.5* and *tie1* expression in pharyngeal clusters undergoing endothelial differentiation. In control embryos, we observed differentiated *tie1*$^{+}$ clusters that had successfully downregulated *nkx2.5* (Fig. 4g,i). In contrast, morphant embryos exhibited persistent expression of *nkx2.5* in clusters that failed to appropriately upregulate *tie1* (Fig. 4h,i), a phenotype that can be rescued by co-injection of full-length zebrafish *nkx2.5* mRNA (Supplementary Fig. 4c-f). Using a double transgenic strain expressing unique fluorescent proteins in the nuclei of either PAA progenitors (red) or endothelial cells (green), we quantified the high degree to which PAA progenitors accumulate at the expense of endothelial cell differentiation in morphant embryos (Fig. 4j-l). Together, these data reveal that Nkx2.5 is dispensable for PAA progenitor specification and maintenence but essential for endothelial differentiation.

To identify potential downstream mediators of *nkx2.5*-dependent endothelial cell differentiation, we examined pharyngeal mesoderm for the expression of two transcription factors, *etsrp71* and *scl*, shown previously to be associated with early specification of the angioblast lineage[21]. At 24 hpf, only *nkx2.5* transcripts were visible in pharygneal clusters (Fig. 5a-d). At 34 hpf, however, we observed four *nkx2.5*$^+$ clusters (Fig. 5e), three *etsrp71*$^+$, *scl*$^+$ clusters (Fig. 5f,g), and two *tie1*$^+$ clusters (Fig. 5h), indicating that *etsrp71* and *scl* transcripts appear subsequent to *nkx2.5* but prior to *tie1* in each cluster. Further, we learned that knocking down *nkx2.5* inhibits the expression of *etsrp71* and *scl* in PAA progenitors (Fig. 5i-m) demonstrating that *nkx2.5* function is required for initating the angioblast program.

To determine if Nkx2.5 is required cell autonomously for PAA vasculogenesis, we generated chimeric embryos via blastula transplantation. Wild-type or *nkx2.5*- deficient donor cells carrying an endothelial transgene [*Tg(kdrl:GFP)*] were transplanted into unlabeled wild-type blastula hosts. Both control and *nkx2.5*-deficient donor cells contributed equally to the body vasculature and endocardium (Fig. 5n,p). However, *nkx2.5*-deficient donor cells failed to contribute to PAA endothelium (Fig. 5o,p), demonstrating that Nkx2.5 is required cell autonomously in PAA progenitors for endothelial differentiation. Moreover, because the hemodynamic environments of the host embryos were unaltered, these findings further solidify the conclusion that Nkx2.5 plays a primary role in PAA establishment.

Our observations support a model (Supplementary Fig. 1) in which *nkx2.5*$^+$ PAA progenitors segregate from cardiac precursors in the heart field and condense into clusters concomitant with pharyngeal segmentation[22]. Clusters 2 and 3 give rise to PAAs 3 and 4, respectively. Further, a small number of *nkx2.5*-expressing heart field progenitors migrate to arches 5 and 6 where naïve mesodermal cells initiate *nkx2.5* expression in the pharynx.

Our findings also highlight a previously unknown and conserved role for Nkx2.5 in blood vessel development. This pro-vasculogenic function of Nkx2.5 was largely unanticipated because previous work demonstrated that misexpression of Nkx2.5 repressed *scl*$^+$ hemangioblast fates in a region of the ALPM anterior to the heart field[23] (Supplementary Fig. 5a, b). However, overexpression of *nkx2.5* did not reduce or expand *tie1*$^+$ PAA endothelial cluster formation in the pharynx (Supplementary Fig. 5c-e), highlighting context dependent roles for Nkx2.5 in angioblast specification. Further, these data demonstrate that PAA progenitor cell differentiation to the endothelial lineage does not require downregulation of *nkx2.5* that otherwise occurs naturally (Fig. 1i-p). Futhermore, FGF signaling was shown to promote ALPM hemangioblast fates at the expense of cardiac fates[23] (Supplementary Fig 5f,g). Inhibition of FGF signaling did not alter PAA progenitor cluster formation or endothelial differentiation indicating a dispensable role for FGF signaling in early PAA morphogenesis (Supplementary Fig. 5h-l). Together, these findings demonstrate that Nkx2.5 actively represses angioblast differentiation early in the ALPM and is required, but not sufficient, for angioblast differentiation later in the pharynx. Although Nkx2.5 targets have been identified within the myocardium[24] and endocardium[25], the *cis*-acting regulatory sequences that are directly activated or repressed by Nkx2.5 during PAA angioblast emergence remain uncharacterized.

Although *nkx2.5* expression in PAA progenitors commences by 14 hpf, Nkx2.5 function is not required until approximately 30+ hpf to activate the PAA vasculogenic program (Fig. 1m-p; Fig. 4). This delay suggests that *nkx2.5*$^{+}$ PAA progenitors integrate a stage- and/or location-specific external cue to cooperatively promote the angioblast fate. However, following endothelial program initiation, *nkx2.5* expression downregulates indicating a specific requirement in promoting the progenitor to angioblast transition. In zebrafish, each PAA wholly derives from *nkx2.5*$^{+}$ cells, and Nkx2.5 is essential cell-autonomously for initiating PAA morphogenesis. However, our lineage tracing and knockout studies in the mouse highlight the possibility that more than one progenitor population contributes to PAA endothelium, as suggested for endocardium[26, 27]. Nonetheless, our work overwhelmingly supports a conserved role for Nkx2-5 in PAA development across vertebrate species. Intriguingly, NKX2.5 mutations in humans can lead to interrupted aortic arch (IAA) type B[28], a great vessel malformation involving left PAA4. Although the etiology of this congenital heart defect has been attributed to abnormal regression of left PAA4, IAA type B might also arise from defects in PAA establishment.

Supplementary Material

Refer to Web version on PubMed Central for supplementary material.

Acknowledgments

We are grateful to S. Paskaradevan and I. Scott for their training in blastula transplantation. We thank C. Kinney for creating Supplementary Figure 1; P. Obregon and T. Cashman for technical assistance in generating the *Tg(nkx2.5:Kaede)* and *Tg(nkx2.5:nZsYellow)* transgenic lines, respectively; W. Goessling for providing *Tg*(*sox17:GFP*) fish; T. North, and L. Zon for providing *Tg*(*kdrl:GFP*) fish; I. Drummond for providing *bon*^{m425} fish; B. Barut and L. Zon for providing bacterial artificial chromosomes (BACs); T. Evans for providing *nkx2.5* plasmid for probe generation; G. Wilkinson and S. Sumanas for providing *etsrp71* plasmid for probe generation; and the MGH Nephrology Division for access to their confocal microscopy facilities. We thank A. Vasilyev for assistance with confocal microscopy. N.P.L is supported by the Harvard Stem Cell Institute Training Grant (5HL087735). B.G.-A. was funded by an American Heart Association (AHA) Post-Doctoral Fellowship (10POST4170037). K.R.N. is funded by a National Research Service Award (5F32HL110627) from the National Heart, Lung and Blood Institute (NHLBI). R.P.H is supported by grants from the National Health and Medical Research Council of Australia (NHMRC; 573732, 573703), Atlantic Philanthropies (19131) and National Heart Foundation of Australia (G08S3718). R.P.H holds an NHMRC Australia Fellowship (573705). This work was funded by awards from the National Heart Lung and Blood Institute (5R01HL096816), American Heart Association (Grant in Aid no.10GRNT4270021), and Harvard Stem Cell Institute (Seed Grant) awards to C.G.B. and the National Heart Lung and Blood Institute (5R01HL111179), the March of Dimes Foundation (FY12-467), and the Harvard Stem Cell Institute (Seed Grant and Young Investigator Award) to C.E.B.

References

1. Congdon ED. Transformation of the aortic arch system during the development of the human embryo. Contributions to Embryology. 1922; 68:49–110.
2. Moore, KL.; Persaud, TVN. The developing human: clinically oriented embryology. 5th. W.B. Saunders; Philadelphia, PA: 1993.
3. Anderson MJ, Pham VN, Vogel AM, Weinstein BM, Roman BL. Loss of unc45a precipitates arteriovenous shunting in the aortic arches. Developmental biology. 2008; 318:258–267. [PubMed: 18462713]
4. Li P, Pashmforoush M, Sucov HM. Mesodermal retinoic acid signaling regulates endothelial cell coalescence in caudal pharyngeal arch artery vasculogenesis. Developmental biology. 2012; 361:116–124. [PubMed: 22040871]

5. Ma Q, Zhou B, Pu WT. Reassessment of Isl1 and Nkx2-5 cardiac fate maps using a Gata4-based reporter of Cre activity. Developmental biology. 2008; 323:98–104. [PubMed: 18775691]
6. Schoenebeck JJ, Keegan BR, Yelon D. Vessel and blood specification override cardiac potential in anterior mesoderm. Developmental cell. 2007; 13:254–267. [PubMed: 17681136]
7. Zhou Y, et al. Latent TGF-beta binding protein 3 identifies a second heart field in zebrafish. Nature. 2011; 474:645–648. [PubMed: 21623370]
8. Serbedzija GN, Chen JN, Fishman MC. Regulation in the heart field of zebrafish. Development. 1998; 125:1095–1101. [PubMed: 9463356]
9. Guner-Ataman B, et al. Zebrafish second heart field development relies on progenitor specification in anterior lateral plate mesoderm and nkx2.5 function. Development. 2013; 140:1353–1363. [PubMed: 23444361]
10. Hami D, Grimes AC, Tsai HJ, Kirby ML. Zebrafish cardiac development requires a conserved secondary heart field. Development. 2011; 138:2389–2398. [PubMed: 21558385]
11. Mosimann C, et al. Ubiquitous transgene expression and Cre-based recombination driven by the ubiquitin promoter in zebrafish. Development. 2011; 138:169–177. [PubMed: 21138979]
12. Hiruma T, Nakajima Y, Nakamura H. Development of pharyngeal arch arteries in early mouse embryo. Journal of anatomy. 2002; 201:15–29. [PubMed: 12171473]
13. Isogai S, Horiguchi M, Weinstein BM. The vascular anatomy of the developing zebrafish: an atlas of embryonic and early larval development. Developmental biology. 2001; 230:278–301. [PubMed: 11161578]
14. Stanley EG, et al. Efficient Cre-mediated deletion in cardiac progenitor cells conferred by a 3′UTR-ires-Cre allele of the homeobox gene Nkx2-5. The International journal of developmental biology. 2002; 46:431–439. [PubMed: 12141429]
15. Novak A, Guo C, Yang W, Nagy A, Lobe CG. Z/EG, a double reporter mouse line that expresses enhanced green fluorescent protein upon Cre-mediated excision. Genesis. 2000; 28:147–155. [PubMed: 11105057]
16. Srinivas S, et al. Cre reporter strains produced by targeted insertion of EYFP and ECFP into the ROSA26 locus. BMC developmental biology. 2001; 1:4. [PubMed: 11299042]
17. Kaufman, MH.; Bard, JBL. The Anatomical Basis of Mouse Development. 1. Academic Press; London: 1999.
18. Targoff KL, Schell T, Yelon D. Nkx genes regulate heart tube extension and exert differential effects on ventricular and atrial cell number. Developmental biology. 2008; 322:314–321. [PubMed: 18718462]
19. Westerfield, M. The zebrafish book A guide for the laboratory use of zebrafish (Danio rerio). 4th. Univeristy of Oregon Press; Eugene OR: 2000.
20. Nicoli S, et al. MicroRNA-mediated integration of haemodynamics and Vegf signalling during angiogenesis. Nature. 2010; 464:1196–1200. [PubMed: 20364122]
21. Sumanas S, Lin S. Ets1-related protein is a key regulator of vasculogenesis in zebrafish. PLoS biology. 2006; 4:e10. [PubMed: 16336046]
22. Schilling TF, Kimmel CB. Segment and cell type lineage restrictions during pharyngeal arch development in the zebrafish embryo. Development. 1994; 120:483–494. [PubMed: 8162849]
23. Simoes FC, Peterkin T, Patient R. Fgf differentially controls cross-antagonism between cardiac and haemangioblast regulators. Development. 2011; 138:3235–3245. [PubMed: 21750034]
24. He A, Kong SW, Ma Q, Pu WT. Co-occupancy by multiple cardiac transcription factors identifies transcriptional enhancers active in heart. Proceedings of the National Academy of Sciences of the United States of America. 2011; 108:5632–5637. [PubMed: 21415370]
25. Ferdous A, et al. Nkx2-5 transactivates the Ets-related protein 71 gene and specifies an endothelial/endocardial fate in the developing embryo. Proceedings of the National Academy of Sciences of the United States of America. 2009; 106:814–819. [PubMed: 19129488]
26. Harris IS, Black BL. Development of the endocardium. Pediatric cardiology. 2010; 31:391–399. [PubMed: 20135106]
27. Milgrom-Hoffman M, et al. The heart endocardium is derived from vascular endothelial progenitors. Development. 2011; 138:4777–4787. [PubMed: 21989917]

28. McElhinney DB, Geiger E, Blinder J, Benson DW, Goldmuntz E. NKX2.5 mutations in patients with congenital heart disease. Journal of the American College of Cardiology. 2003; 42:1650–1655. [PubMed: 14607454]

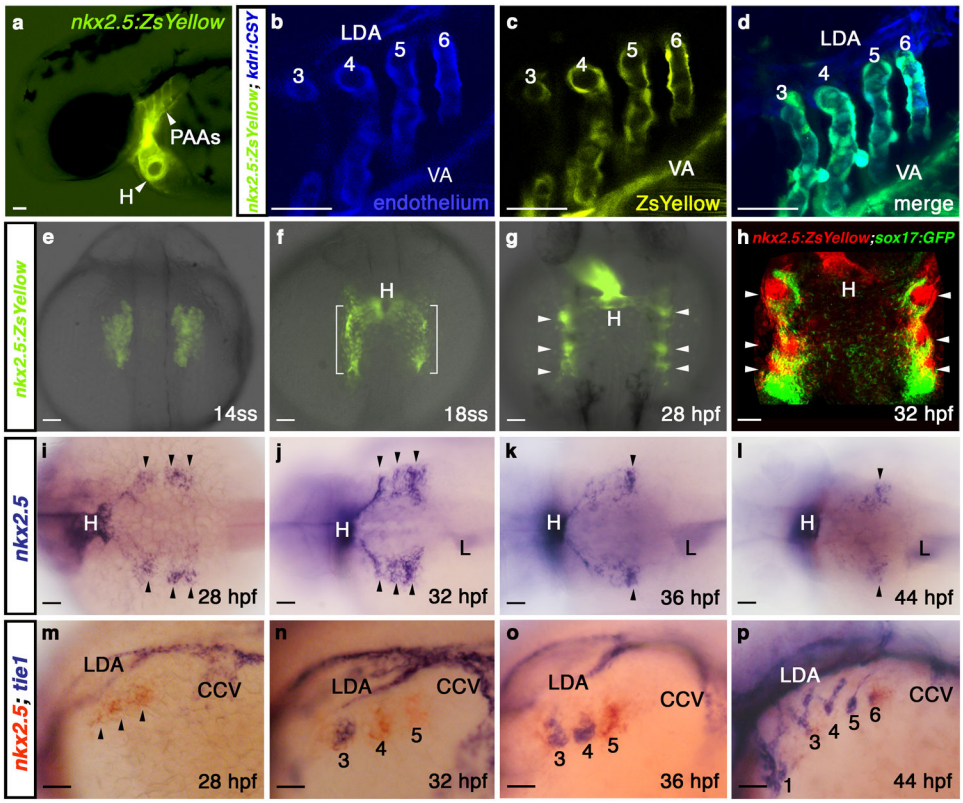

Figure 1. *nkx2.5* is expressed in presumptive PAA endothelial progenitors

a, *Tg(nkx2.5:ZsYellow)* embryo at 60 hpf exhibiting fluorescence in the heart and PAAs. **b-d**, *Tg(nkx2.5:ZsYellow); Tg(kdrl:CSY)* embryo at 60 hpf with overlapping yellow and blue fluorescence in the endothelium of PAAs 3-6 and the VA. The LDA exhibits blue fluorescence exclusively. **e-g**, ZsYellow fluorescence in *Tg(nkx2.5:ZsYellow)* embryos at 14ss (**e**), 18ss (**f**), and 28 hpf (**g**). Brackets and arrowheads highlight non-cardiogenic *nkx2.5*$^{+}$ cells in the pharynx. **h**, *Tg(nkx2.5:ZsYellow); Tg(sox17:GFP)* embryo at 32 hpf with *nkx2.5*$^{+}$ pharyngeal cells (red) and *sox17*$^{+}$ pharyngeal endoderm (green); **i-l**, *in situ* hybridization time-course of *nkx2.5* expression in the pharynx. Arrowheads mark *nkx2.5*$^{+}$ pharyngeal clusters. **m-p**, Double *in situ* hybridization time-course of *nkx2.5* (red) and *tie1* (blue) expression. PAA1 (labelled in **p**) forms earlier in development and never expresses *nkx2.5*. *tie1*$^{+}$ clusters are numbered according to the mature PAA they derive. **a-d**, **m-p**, lateral views, anterior left; **e-h**, dorsal views, anterior up; **i-l**, dorsal views, anterior left; **a-p**, *n*>20 embryos per group. Abbr: VA, ventral aorta; LDA, lateral dorsal aorta; ss, somite-stage; hpf, hours post-fertilization; H, heart; L, liver; CCV, common cardinal vein.

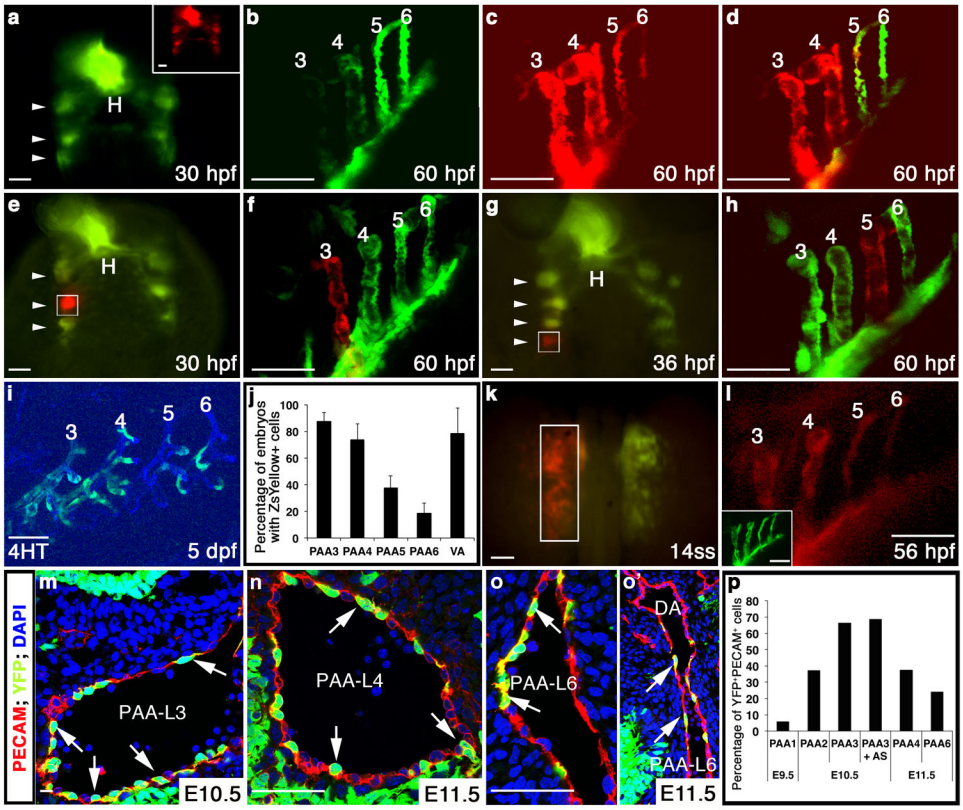

Figure 2. *nkx2.5*$^{+}$progenitors give rise to PAA endothelium in zebrafish and mouse

a-d, *Tg(nkx2.5:Kaede)* embryo at 30 hpf before (green) and after (red, inset) pan-photoconversion (*n*=3). Arrowheads highlight Kaede^{+} pharyngeal clusters. At 60 hpf, embryos were imaged in the green (**b**) and red (**c**) channels and these images were merged (**d**). **e-h**, Localized Kaede photoconversion of cluster 2 (**e**, white box, *n*=2) or 4 (**g**, white box, *n*=2) at the indicated developmental stages. Merged red and green images of the PAAs in the same embryos at 60 hpf are shown in (**f**) and (**h**). **i**, ZsYellow reporter fluorescence in PAAs 3-6 at 5 dpf in a *Tg(nkx2.5:CreER*^{T2}*); Tg(kdrl:CSY)* embryo treated with 4HT from 10-13 hpf. **j**, Graph showing the average percentages of embryos with ZsYellow^{+} reporter fluorescence in each PAA and the VA across four experimental repliates (*n*=160). Error bars indicate one standard deviation. **k**, Left ALPM of a *Tg(nkx2.5:Kaede)* embryo photoconverted (white box) at 14ss and subsequently imaged in the red (**l**) and green channels (inset), (*n*=5). **m-o′**, *Nkx2-5*^{IRESCre}; *ROSA*^{YFP} embryos co-stained with PECAM1 (red) and DAPI (blue). Arrows indicate YFP^{+}/PECAM^{+} lineage traced endothelial cells. **o′**, Left PAA 6 junction with DA. **p**, Graph depicting the average percentage of endothelial cells (PECAM1^{+}) co-expressing YFP within each PAA. Cells counted across two embryos: E9.5 (PAA 1, *n*=244), E10.5 (PAA 2, *n*=216, PAA 3, *n*=1357, PAA3 + aortic sac, *n*=642), and E11.5 (PAAs 4, *n*=511 and 6, *n*=649). **a**,**e**,**g**,**k**, dorsal views, anterior up; **b-d**,**f**,**h**,**i**,**l**, lateral views, anterior left. Scale bar = 50μm. Abbr: hpf, hours post-fertilization; dpf, days post-fertilization; H, heart; AS, aortic sac; DA, dorsal aorta; PAA number and left (L) and right (R) designations indicated.

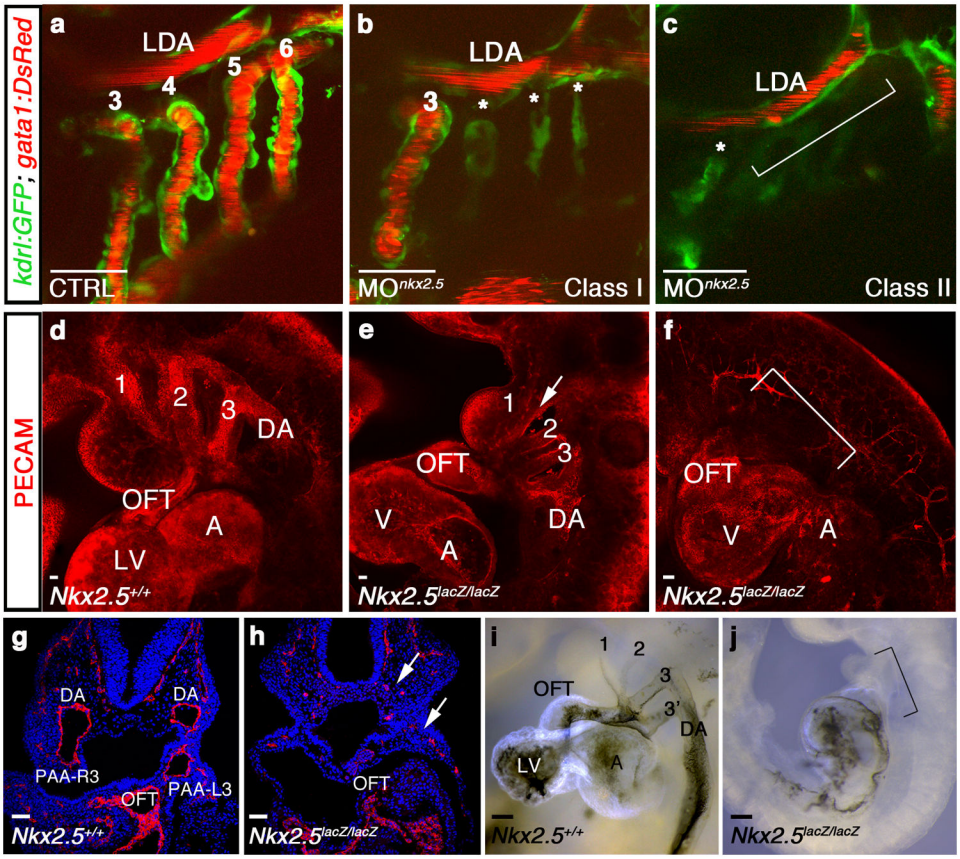

Figure 3. Nkx2.5 is required for vertebrate PAA formation

a-c, *Tg(kdrl:GFP); Tg(gata1:DsRed)* zebrafish embryos with green endothelial cells and red erythrocytes at 60 hpf. **a**, Control (CTRL) embryo with patent PAAs 3-6 and LDA (*n*=60/60). **b**, Class I *nkx2.5* morphant (MO$^{nkx2.5}$) in which one (shown) or two PAAs support blood flow. Asterisks label malformed PAAs (*n*=88/116). **c**, Class II *nkx2.5* morphant lacking patent PAAs (bracket, *n*=22/116). **d-f**, Whole mount control (**d**) or *Nkx2-5* null (**e**,**f**) mouse embryos stained for PECAM1 (red) at E9.5 (*n*=5 per group). *Nkx2-5* null embryos displayed disrupted PAAs 1-3 with residual isolated endothelial cells (arrow, **e**) or a complete absence of PAAs altogether (bracket, **f**). **g**,**h**, Sections through control and *Nkx2-5* null embryos stained with PECAM (red) and DAPI (blue). Arrow shows residual endothelial cells (**h**). **i**,**j**, Ink injections in control and *Nkx2-5* null animals at E9.5 (*n*=5 per group). Bracket in **j** indicates absence of flow through the mutant OFTs. **a-c**, lateral views, anterior left; **d-f**, **i**,**j**, lateral views, anterior up; **g**,**h**, coronal sections. Scale bar = 50μm. Abbr: LDA, lateral dorsal aorta; DA, dorsal aorta; OFT, outflow tract; LV, left ventricle; A, atrium; V, ventricle; PAA number and left (L) and right (R) designations indicated.

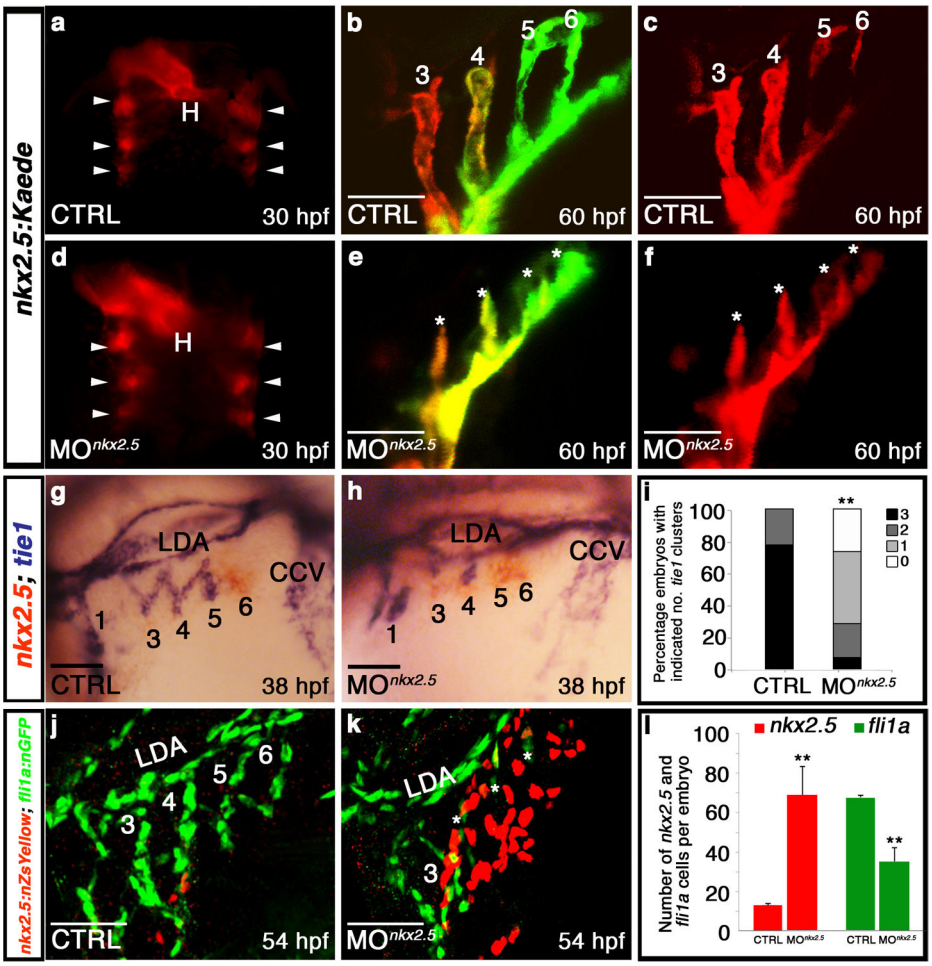

Figure 4. Nkx2.5 is required for PAA progenitor cell differentiation

a-f, Control (*n*=3) and *nkx2.5* morphant (*n*=5) *Tg(nkx2.5:Kaede)* embryos were pan-photoconverted at 30 hpf (**a**,**d**). Arrowheads show Kaede^{+} pharyngeal clusters. At 60 hpf, embryos were imaged in red and green channels with red (**c**,**f**) and merged (**b**,**e**) images shown. Asterisks (**e,f**) mark abnormal PAAs 3-6 in *nkx2.5* morphant embryos. **g**,**h**, *nkx2.5* (red) and *tie1* (blue) transcripts evaluated by double *in situ* hybridization in control (**g**) and morphant (**h**) embryos. **i**, Quantification of *tie1*$^{+}$ clusters in control (*n*=95) and *nkx2.5* morphant (*n*=42) embryos across three experimental replicates; two-tailed *t* test ***P*=0.0001. **j**,**k**, Control and nkx2.5 morphant *Tg(nkx2.5:nZsYellow); Tg(fli1a:nEGFP)* embryos showing *nkx2.5*$^{+}$ PAA progenitors (red) and *fli1a*$^{+}$ endothelial cells (green) detected by immunohistochemistry. **l**, Quantification of *nkx2.5*$^{+}$ and *fli1a*$^{+}$ cells in control (*n*=4) and *nkx2.5* morphant (*n*=4) embryos; Error bars indicate one standard deviation, two-tailed *t* test *nkx2.5* ***P*=0.0073, *fli1a* ***P*=0.0008 across three independent experiments. Scale bar = 50μm. **a**,**d**, dorsal views, anterior up; **b**,**c**,**e**,**f**,**g**,**h**,**j**,**k**, lateral views, anterior left; PAA numbers indicated.

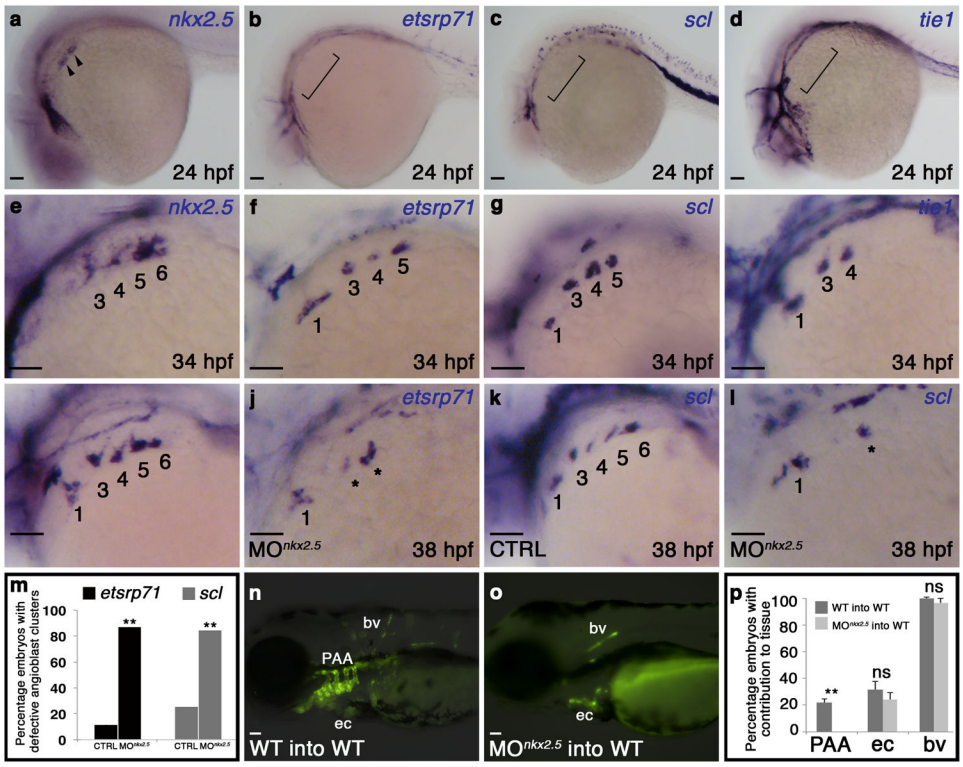

Figure 5. Cell-autonomous requirement for Nkx2.5 in promoting the PAA progenitor to angioblast transition

a-**h**, *in situ* hybridization analysis of *nkx2.5*(**a**,**e**), *etsrp71*(**b**,**f**), *scl*(**c**,**g**), and *tie1*(**d**,**h**) at 24 (**a**-**d**) and 34 (**e**-**h**) hpf. **i**-**l***etsrp*(**i**,**j**) and *scl*(**k**,**l**) transcripts evaluated by *in situ* hybridization in control (CTRL; **i**,**k**) and *nkx2.5* morphant (MO$^{nkx2.5;}$**j**,**l**) embryos, asterisks mark abnormal PAAs 3-6, numbers are quantified in **m**. *(etsrp* CTRL *n*=61, MO$^{nkx2.5}$ *n*=53, two-tailed *t* test ***P*=0.001 across two independent experiments; *scl* CTRL *n*=106, MO$^{nkx2.5}$ *n*=116, two-tailed *t* test ***P*=0.001 across two independent experiments). **n**-**p**, WT (**n**) and MO$^{nkx2.5}$(**o**) donor-derived GFP^{+} PAA endothelium in unlabelled WT hosts. **p**, Quantification of host embryos showing GFP^{+} donor cells from WT (*n*=208) or MO$^{nkx2.5}$ (*n*=86) embryos in the PAAs, endocardium (ec), and body vasculature (bv). Fishers exact test, PAA two tailed ***P*=0.0001; ec two-tailed *P*=0.3239 (not significant, ns); bv two-tailed *P*=0.2710, across four independent experiments. Scale bar = 50μm. **a**-**l**, lateral views, anterior left; PAA islands indicated; **a**-**h** *n*>20 embryos per group; **m**,**p**, Error bars indicate one standard deviation.